0022-3565/11/3391-35–44$25.00
THE JOURNAL OF PHARMACOLOGY AND EXPERIMENTAL THERAPEUTICS
JPET 339:35–44, 2011

Vol. 339, No. 1
182220/3714583
Printed in U.S.A.

Facilitation of Hippocampal Synaptogenesis and Spatial Memory by C-Terminal Truncated Nle[1]-Angiotensin IV Analogs

Caroline C. Benoist, John W. Wright, Mingyan Zhu, Suzanne M. Appleyard, Gary A. Wayman, and Joseph W. Harding

Department of Veterinary and Comparative Anatomy, Pharmacology and Physiology (C.C.B., J.W.W., M.Z., S.M.A., G.A.W., J.W.H.), Program in Neuroscience (C.C.B., J.W.W., M.Z., S.M.A., G.A.W., J.W.H.), Program in Biotechnology (J.W.W., J.W.H.), and Department of Psychology (J.W.W., J.W.H.), Washington State University, Pullman, Washington

Received April 7, 2011; accepted June 29, 2011

ABSTRACT

Angiotensin IV (AngIV; Val[1]-Tyr[2]-Ile[3]-His[4]-Pro[5]-Phe[6])-related peptides have emerged as potential antidementia agents. However, their development as practical therapeutic agents has been impeded by a combination of metabolic instability, poor blood-brain barrier permeability, and an incomplete understanding of their mechanism of action. This study establishes the core structure contained within norleucine[1]-angiotensin IV (Nle[1]-AngIV) that is required for its procognitive activity. Results indicated that Nle[1]-AngIV-derived peptides as small as tetra- and tripeptides are capable of reversing scopolamine-induced deficits in Morris water maze performance. This identification of the active core structure contained within Nle[1]-AngIV represents an initial step in the development of AngIV-based procognitive drugs. The second objective of the study was to clarify the general mechanism of action of these peptides by assessing their ability to affect changes in dendritic spines. A correlation was observed between a peptide's procognitive activity and its capacity to increase spine numbers and enlarge spine head size. These data suggest that the procognitive activity of these molecules is attributable to their ability to augment synaptic connectivity.

Introduction

Until recently the hexapeptide angiotensin IV (AngIV; Val[1]-Tyr[2]-Ile[3]-His[4]-Pro[5]-Phe[6]) was considered a biologically inactive metabolite of the octapeptide angiotensin II (for reviews, see von Bohlen und Halbach and Albrecht, 2006; Fyhrquist and Saijonmaa, 2008; Vanderheyden, 2009). However, multiple reports indicate that AngIV and several AngIV analogs can facilitate long-term potentiation, learning, and memory consolidation (Braszko et al., 1988; Wright et al., 1999; Kramár et al., 2001; Lee et al., 2004a), increase cerebral blood flow (Kramár et al., 1997), and provide neuroprotection (Faure et al., 2006). Of most importance, the acute application of one of these analogs, Nle[1]-AngIV, reverses deficits in dementia models induced by 1) treatment with the cholinergic muscarinic receptor antagonist scopolamine (Pederson et al., 2001), 2) kainic acid injections into the hippocampus (Stubley-Weatherly et al., 1996), 3) perforant path cuts (Wright et al., 1999), and 4) ischemia resulting from transient four-vessel occlusion (Wright et al., 1996). Consistent with these behavioral and electrophysiological results, brain binding sites for ^{125}I-AngIV have been autoradiographically localized in structures known to mediate cognitive processing including the neocortex, hippocampus, and basal nucleus of Meynert (Harding et al., 1992; Chai et al., 2000; Wright and Harding, 2008). It should be noted that the AT_1 angiotensin receptor subtype may also contribute to the cognitive effects of AngIV (De Bundel et al., 2010).

Not surprisingly, AngIV-based pharmaceutical agents have been suggested as antidementia therapeutic agents (Mustafa et al., 2001; von Bohlen und Halbach, 2003; Gard, 2004, 2008; De Bundel et al., 2008; Wright and Harding, 2008). Despite promising behavioral effects in animal models

This work was supported by the National Institutes of Health National Institute of Mental Health [Grant MH086032]; the Edward E. and Lucille I. Lainge Endowment for Alzheimer's Research, State of Washington Initiative [Measure 171] (to J.W.W.); and the Hope for Depression Research Foundation (to G.A.W.).

J.W.W. and J.W.H. are the cofounders of Pacific Northwest Biotechnology, LLC and hold stock in this company, which is involved in the development of antidementia drugs.

Article, publication date, and citation information can be found at http://jpet.aspetjournals.org.

doi:10.1124/jpet.111.182220.

ABBREVIATIONS: AngIV, angiotensin IV; Nle, norleucine; BBB, blood-brain barrier; aCSF, artificial cerebrospinal fluid; mRFP, monomeric red fluorescent protein; DIV, days in vitro; PBS, phosphate-buffered saline; α-VGLUT1, vesicular glutamate transporter; EPSC, excitatory postsynaptic current; mEPSC, mini-excitatory postsynaptic current; ANOVA, analysis of variance; BDNF, brain-derived neurotrophic factor; LTP, long-term potentiation.

of dementia, two critical physiochemical properties, namely lack of metabolic stability and inability to penetrate the blood-brain barrier (BBB), have precluded drug development. This later limitation of AngIV-related peptides results from considerations of molecular size, overall hydrophobicity, and hydrogen-bonding potential as reflected by the size of the encompassing hydration sphere. In an initial attempt to transform Nle^1-AngIV into an efficacious drug, the present investigation examined the procognitive activity of a series of C-terminal truncated peptides derived from Nle^1-AngIV. We initially focused on reducing the size of the agonist to determine the smallest active derivative. The decision to work from the C terminus was based on a previous study indicating that removal of the N-terminal Nle resulted in a loss of cognitive-enhancing activity (Wright et al., 1999). To assess procognitive activity, rats were made amnesic with scopolamine, followed by treatment with Nle^1-AngIV or one of the C-terminal truncated analogs, and tested for spatial learning using the Morris water maze task. This scopolamine preparation yields a widely accepted animal model of the spatial memory dysfunction similar to that observed in patients with early- to middle-stage Alzheimer's disease (Fisher et al., 2003).

One possible explanation for the procognitive activity of AngIV-related molecules is a capacity to expand synaptic connectivity and augment synaptic communication. Thus, the second goal of this study was to evaluate the ability of these truncated peptides to alter dendritic spine architecture and further determine whether this capability correlated with the cognitive-enhancing capacity of the molecule. The decision to examine the influence of these peptides on dendritic spine numbers, size, length, and spine association with presynaptic markers was based on previous findings that functionally linked these dendritic properties to cognitive performance (for review, see Kennedy et al., 2005).

Materials and Methods

Animals and Surgery. Male Sprague-Dawley rats (Taconic-derived) weighing 390 to 450 g were maintained with free access to water and food (Harlan Teklad F6 rodent diet; Harlan Teklad, Madison, WI) except during the night before surgery when food was removed. Each animal was anesthetized with ketamine hydrochloride plus xylazine (100 and 2 mg/kg i.m., respectively; Phoenix Scientific, St. Joseph, MO, and Moby, Shawnee, KS). An intracerebroventricular guide cannula (PE-60; Clay Adams, Parsippany, NY) was stereotaxically positioned (model 900; David Kopf Instruments, Tujunga, CA) in the right hemisphere using flat skull coordinates 1.0 mm posterior and 1.5 mm lateral to bregma. The guide cannula measured 2.5 cm in overall length and was prepared with a heat bulge placed 2.5 mm from its beveled tip, which acted as a stop to control the depth of penetration. Once in position, the cannula was secured to the skull with two stainless-steel screws and dental cement. Postoperatively the animals were housed individually in an American Association for Assessment and Accreditation for Laboratory Animal Care-approved vivarium maintained at 22 ± 1°C on a 12-h alternating light/dark cycle initiated at 6:00 AM. All animals were handled gently for 5 min/day during the 5 to 6 days of postsurgical recovery. Histological verification of cannula placement was accomplished by the injection of 5 μl of Fast Green dye via the guide cannula after the completion of behavioral testing. Correct cannula placement was evident in all rats used in this study.

Behavioral Testing. The water maze consisted of a circular tank painted black (diameter 1.6 m; height 0.6 m), filled to a depth of 26 cm with 26–28°C water. A black circular platform (diameter, 12 cm; height, 24 cm) was placed 30 cm from the wall and submerged 2 cm below the water surface. The maze was operationally sectioned into four equal quadrants designated northwest, northeast, southwest, and southeast. For each rat, the location of the platform was randomly assigned to one of the quadrants and remained fixed throughout the duration of training. Entry points were at the quadrant corners (i.e., north, south, east, and west) and were pseudo-randomly assigned such that each trial began at a different entry point than the preceding trial. Three of the four testing room walls were covered with extra-maze spatial cues consisting of different shapes (circles, squares, and triangles) and colors. The swimming path of the animals was recorded using a computerized video tracking system (Chromotrack; San Diego Instruments, San Diego, CA). The computer displayed total swim latency and swim distance. Swim speed was determined from these values.

Each member of the treatment groups received an intracerebroventricular injection of scopolamine hydrobromide [70 nmol in 2 μl of artificial cerebrospinal fluid (aCSF) over a duration of 20 s] 20 min before testing followed by Nle^1-AngIV or one of the analogs (in 2 μl of aCSF) 5 min before testing. Control groups received scopolamine or aCSF 20 min before testing followed by aCSF 5 min before testing. The behavioral testing protocol has been described in detail previously (Wright et al., 1999). In brief, acquisition trials were conducted on 8 consecutive days with five trials/day. On the first day of training, the animal was placed on the platform for 30 s before the first trial. Trials commenced with the placement of the rat facing the wall of the maze at one of the assigned entry points. The rat was allowed a maximum of 120 s to locate the platform. Once the animal located the platform, it was permitted a 30-s rest period on the platform. If the rat did not find the platform, the experimenter placed the animal on the platform for the 30-s rest period. The next trial commenced immediately after the rest period.

After day 8 of acquisition training, one additional trial was conducted during which the platform was removed (probe trial). The animal was required to swim the entire 120 s to determine the persistence of the learned response. Total time spent within the target quadrant where the platform had been located during acquisition and the number of crossings of that quadrant were recorded. Upon completion of each daily set of trials, the animal was towel-dried and placed under a 100-W lamp for 10 to 15 min and then returned to its home cage.

Compounds and Peptide Synthesis. Scopolamine hydrobromide was purchased from Sigma-Aldrich (St. Louis, MO). The peptides were synthesized on methylated 1% divinylbenzene cross-linked polystyrene resins substituted with the protected carboxyl-terminal amino acid in a semiautomated peptide synthesizer (Endeavor 90; AAPPTec, Louisville, KY). Amino acids were activated with *l*-ethyl-3-(3-dimethylaminopropyl)-carbodiimide, and coupling was monitored for completeness with the Kaiser ninhydrin test. Crude peptides were cleaved from the resin and de-protected using anhydrous hydrogen fluoride (HF) containing 10% anisole at 0°C for 45 min. The HF and anisole were removed under vacuum, and the resin was washed with anhydrous diethyl ether. Peptides were extracted with 10% acetic acid and lyophilized. Finally, the crude compounds were purified by reverse-phase high-performance liquid chromatography in two steps on a preparative Dynamax C-18 21.4 mm × 25 cm column (Rainin Instruments, Woburn, MA). The peptides were first separated isocratically using an appropriate ratio of buffer A and solvent B (typically between 14 and 1%) at 10 ml/min. Buffer A consisted of 180 mM triethylamine phosphate, pH 3.0. Solvent B was acetonitrile. The absorbance of the eluted material was monitored at 210, 254, and 280 nm. The collected peak was concentrated under a stream of nitrogen and further purified using a gradient elution: 0 to 30% B over 26 min, 30 to 30% B for 15 min, and 30 to 50% B over 15 min at 10 ml/min (buffer A: 0.1% trifluoroacetic acid in H_2O; solvent B: 0.1% trifluoroacetic acid-acetonitrile). Purities of the collected peaks were assessed by monitoring the ratio

of 280- and 215-nm absorbance across the collected peak. The purified peptide was lyophilized and stored desiccated at −20°C. Final purity was determined by compositional amino acid analysis and high-performance liquid chromatography. All peptide purities were determined to be >98%, whereas overall peptide content ranged from 70 to 75% with salts making up the remaining content. Before use, each compound was prepared in sterile aCSF at the appropriate dose per 2 μl of aCSF and stored at −20°C in siliconized sealed culture tubes.

Hippocampal Cell Culture Preparation. Hippocampal neurons (2×10^5 cells/cm^2) were cultured from P1 Sprague-Dawley rats on plates coated with poly-L-lysine from Sigma-Aldrich (molecular weight 300,000). Hippocampal neurons were maintained in Neurobasal A medium from Invitrogen (Carlsbad, CA) supplemented with B27 (Invitrogen) and 0.5 mM L-glutamine and 5 mM cytosine-D-arabinofuranoside (Sigma-Aldrich) added at 2 days in vitro. Hippocampal neurons were then cultured a further 3 to 7 days, at which time they were either transfected or treated with various pharmacological reagents as described in Wayman et al. (2008).

Transfection. Neurons were transfected with mRFP-β-actin on day in vitro (DIV) 6 using Lipofectamine 2000 (Invitrogen) according to the manufacturer's protocol. This protocol yielded the desired 3 to 5% transfection efficiency, thus enabling the visualization of individual neurons. Higher efficiencies obscured the dendritic arbor of individual neurons. Expression of fluorescently tagged actin allowed clear visualization of dendritic spines, because dendritic spines are enriched in actin. On DIV7, the cells were treated with vehicle (H_2O) or peptides (as described in the text) added to media. On DIV12, the neurons were fixed (4% paraformaldehyde, 3% sucrose, 60 mM PIPES, 25 mM HEPES, 5 mM EGTA, and 1 mM $MgCl_2$, pH 7.4) for 20 min at room temperature and mounted.

Slides were dried for at least 20 h at 4°C, and fluorescent images were obtained with Slidebook 4.2 Digital Microscopy Software driving an Olympus IX81 inverted confocal microscope (Olympus Optical, Tokyo, Japan) with a 60× oil immersion lens, numerical aperture 1.4, and resolution 0.280 μm. Dendritic spine density was measured on primary and secondary dendrites at a distance of at least 150 μm from the soma. Five 50-μm long segments of dendrites from at least 10 neurons were analyzed for each data point reported. Each experiment was repeated at least three times using independent culture preparations. Dendrite length was determined using ImageJ 1.41o (National Institutes of Health, Bethesda, MD) and the neurite tracing program Neuron J (Meijering et al., 2004). Spines were manually counted.

Immunocytochemistry. Transfected neurons were treated and fixed as described above. After fixation, cells were rinsed in PBS and permeabilized with 0.1% Triton X-100 detergent (Bio-Rad Laboratories, Hercules, CA), followed by two rinses in PBS, and blocked with 8% bovine serum albumin (Serological Corp., Norcross, GA) in PBS for 1 h. Cells were again rinsed with PBS, followed by a 24-h incubation period with anti-α-VGLUT1 (Synaptic Systems, Goettingen, Germany) or anti-synapsin (Synaptic Systems), following the manufacturer's protocol, at 4°C. Then, cells were rinsed twice with PBS, incubated in Alexa Fluor 488 goat-anti-mouse IgG following the manufacturer's protocol (Invitrogen) for 2 h at room temperature, rinsed again with PBS, and mounted with ProLong Gold anti-fade reagent (Invitrogen). Imaging and analysis were performed as described above.

Whole-Cell Recordings. Patch-clamp experiments were performed on mRFP-β-actin-transfected cultured hippocampal neurons with PBS (vehicle control) or 1 pM Nle^1-AngIV pretreatment. Recordings were made on DIV12 to DIV14. The culture medium was exchanged by an extracellular solution containing 140 mM NaCl, 2.5 mM KCl, 1 mM $MgCl_2$, 3 mM $CaCl_2$, 25 mM glucose, and 5 mM HEPES; pH was adjusted to 7.3 with KOH, and osmolality was adjusted to 310 mOsM. Cultures were allowed to equilibrate in a recording chamber mounted on an inverted microscope (IX-71; Olympus Optical) for 30 min before recording. Transfected cells were visualized with fluorescence (Olympus Optical). Recording pipettes were pulled (P-97 Flaming/Brown micropipette puller; Sutter Instrument Company, Novato, CA) from standard-wall borosilicate glass without filament (o.d. = 1.5 mm; Sutter Instrument Company). The pipette-to-bath d.c. resistance of patch electrodes ranged from 4.0 to 5.2 MΩ, and they were filled with an internal solution of the following composition: 25 mM CsCl, 100 mM $CsCH_3O_3S$, 10 mM phosphocreatine, 0.4 mM EGTA, 10 mM HEPES, 2 mM $MgCl_2$, 0.4 mM Mg-ATP, and 0.04 mM Na-GTP; pH was adjusted to 7.2 with CsOH, and osmolality was adjusted to 296 to 300 mOsM. Miniature EPSCs (mEPSCs) were isolated pharmacologically by blocking GABA receptor chloride channels with picrotoxin (100 μM; Sigma-Aldrich), blocking glycine receptors with strychnine (1 μM; Sigma-Aldrich), and blocking action potential generation with tetrodotoxin (500 nM; Tocris Bioscience, Ellisville, MO). Recordings were obtained using a Multiclamp 700B amplifier (Molecular Devices, Sunnyvale, CA). Analog signals were low-pass Bessel-filtered at 2 kHz, digitized at 10 kHz through a Digidata 1440A interface (Molecular Devices), and stored in a computer using Clampex 10.2 software (Molecular Devices). The membrane potential was held at −70 mV at room temperature (25°C) during a period of 0.5 to 2 h after removal of the culture from the incubator. Liquid junction potentials were not corrected. Data analysis was performed using Clampfit 10.2 software (Molecular Devices) and Mini-Analysis 6.0 software (Synaptosoft, Decatur, GA). The criteria for a successful recording included an electrical resistance of the seal between the outside surface of the recording pipette and the attached cell >2 GΩ and neuron input resistance >240 MΩ. The mEPSCs had a 5-min recording time.

Statistical Analyses. Morris water maze data sets, consisting of mean latencies and path distances to find the platform during each daily block of five trials, were calculated for each animal for each day of acquisition. One-way ANOVAs were used to compare group latencies swum on days 1, 4, and 8 of training. Past experience with this task has indicated these days to be representative of overall performance. Data collected during the probe trials (time spent in the target quadrant and entries into the target quadrant) were also analyzed using one-way ANOVAs. Significant effects were further analyzed by a Newman-Keuls post hoc test with a level of significance set at $p < 0.05$.

One-way ANOVA was used to analyze the dendritic spine results and significant effects were analyzed by Tukey post hoc test. Linear regression analysis was used to determine the correlation between spine characteristics and latency to find the platform in the water maze task. Multiple comparisons of electrophysiological results were made using a one-way ANOVA followed by a Newman-Keuls post hoc test with a level of significance set at $p < 0.05$. Numerical data are expressed as means ± S.E.M.

Results

Behavioral Testing. Spatial learning was assessed using the Morris water maze task in which rats learn to locate a submerged platform by using extra-maze cues. Figure 1 presents the mean search latencies for days 1 to 8 of training. Figure 1A provides contrasting learning (latency) profiles for fully functional control rats (aCSF-vehicle followed by aCSF), and memory-impaired rats (scopolamine followed by aCSF). Figure 1B shows the results from rats pretreated with scopolamine and subsequently treated with Nle^1-AngIV or the following Nle^1-AngIV-related peptides: Nle^1-YIHP (pentapeptide), Nle^1-YIH (tetrapeptide), Nle^1-YI (tripeptide), or Nle^1-Y (dipeptide). Rats from each of these peptide-treated groups, except the Nle^1-Y group, exhibited improved latencies to find the platform compared with those for the scopolamine followed by aCSF group. None of the experimental groups differed from the scopolamine deficit group on day 1

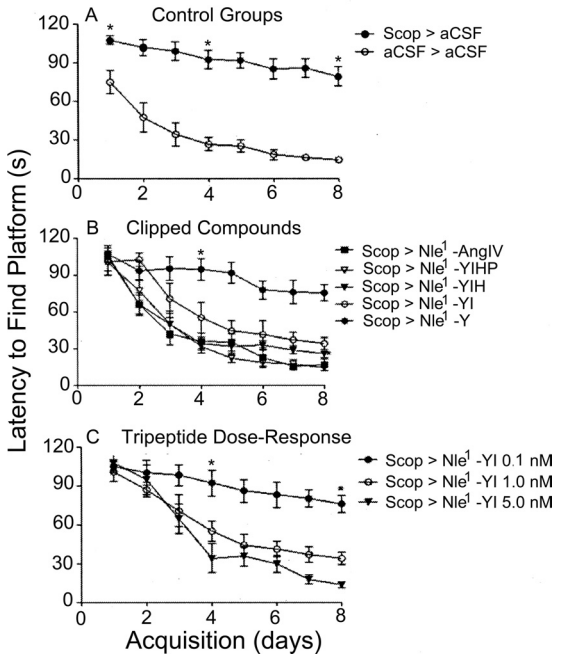

Fig. 1. Group latencies to find the submerged platform in the Morris water maze task of spatial memory. A, data from the two groups representing the maximum scopolamine-induced disruption of acquisition (Scop > aCSF) and the most efficient acquisition expected during training (aCSF > aCSF) are presented. B, data from five groups of rats ($n = 8$ each), pretreated with intracerebroventricular scopolamine (70 nmol in 2 μl of aCSF) 20 min before training followed by the intracerebroventricular infusion of the designated analog (1 nmol in 2 μl of aCSF) 5 min before daily training. C, additional groups were pretreated with intracerebroventricular scopolamine followed by 0.1, 1, or 5 nmol of Nle^1-YI (in 2 μl of aCSF). Mean ± S.E.M.; *, $p < 0.01$.

except the vehicle control group, which received no scopolamine (mean latency = 74.8 ± 9.1 s; $F = 2.51$, $df = 6/49$, $p < 0.05$). All peptide-treated groups, except the Nle^1-Y-treated group, began to separate from the scopolamine group by day 3. By day 4 of acquisition, the groups had clearly sorted out into those exhibiting progressively improving search patterns (control, scopolamine/Nle^1-AngIV, scopolamine/Nle^1-YIHP, scopolamine/Nle^1-YIP, and scopolamine/Nle^1-YI) versus the remaining two groups (scopolamine/Nle^1-Y and scopolamine/aCSF), which performed poorly ($F = 11.75$, $df = 6/49$, $p < 0.0001$). The last two groups continued to perform poorly through day 8 of testing and were significantly different from the other groups regarding latency to find the platform ($F = 28.61$, $df = 6/49$, $p < 0.0001$). The vehicle control (aCSF followed by aCSF), the Nle^1-AngIV, the Nle^1-YIHP, and the Nle^1-YIH groups were adept at finding the platform and did not differ on day 8. Although members of the Nle^1-YI group performed reasonably well on day 8, they did require significantly more time to find the platform than the vehicle control (aCSF followed by aCSF), Nle^1-AngIV, and Nle^1-YIHP groups.

Given the above results, we were particularly interested in further testing the Nle^1-YI compound and reasoned that a higher dose may improve performance. Thus, we tested three additional groups using doses of 0.1, 1, and 5 nmol after scopolamine pretreatment (Fig. 1C). The dose of 5 nmol yielded an acquisition curve that was not statistically different from those seen with Nle^1-YIH, Nle^1-YIHP, and Nle^1-AngIV (Fig. 1B).

After acquisition training on day 8, one additional trial was initiated during which no platform was present in the maze. This "probe" trial assesses the time each rat spends searching for the missing platform in its original target quadrant and is considered a gauge of the strength of the learned response (Lopez et al., 2009), thus providing a second measure of the cognitive-enhancing properties of these Nle^1-AngIV-related peptides. Figure 2A offers a comparison between control rats and those impaired by scopolamine application. These data indicate that control rats spent 175% more time in the target quadrant than impaired rats ($F = 37.22$, df 6/49, $p < 0.0001$). Animals treated with scopolamine followed by aCSF (Fig. 2A) spent 22.3 ± 2.8 s in the target quadrant

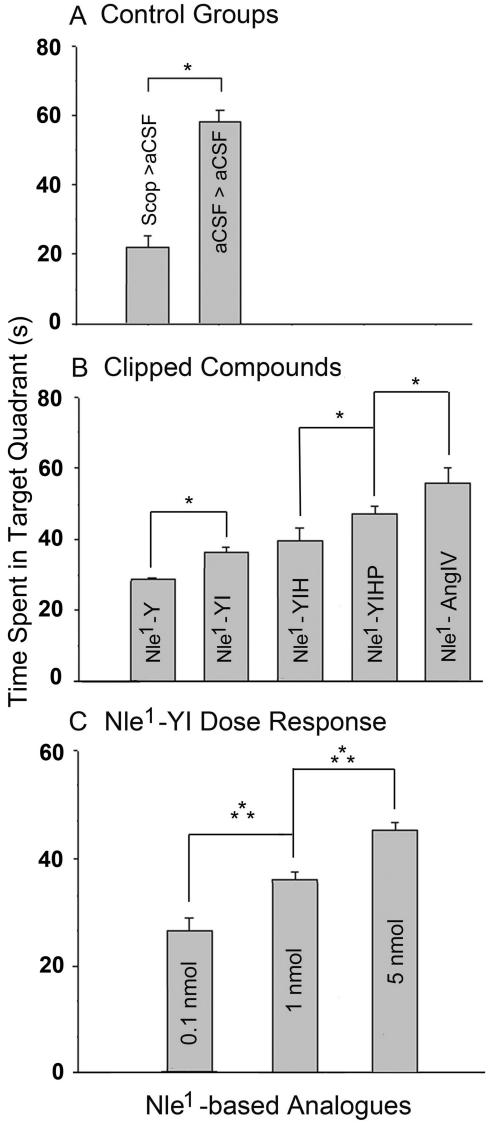

Fig. 2. Day 8 probe trials by each experimental group. Time spent in the target quadrant was recorded for each experimental group. A, the scopolamine (scop) > aCSF group performed below chance level (30 s) and was significantly different from the aCSF > aCSF control group ($p > 0.001$). B, the scopolamine followed by 1 nmol of Nle^1-YI, Nle^1-YIH, and Nle^1-YIHP groups spent significantly more time in the target quadrant than the Nle-Y-treated group ($p < 0.05$). The group treated with Nle^1-AngIV spent significantly more time in the target quadrant than any of the other groups ($p > 0.05$). C, the group pretreated with scopolamine followed by 5 nmol of Nle^1-YI spent significantly more time in the target quadrant than the 1-nmol group, which in turn spent more time than the 0.1-nmol group. Mean ± S.E.M.; *, $p < 0.01$.

and differed from the Nle[1]-Y-treated rats (Fig. 2B), which spent a mean of 28.7 ± 0.6 s in the target quadrant. Although statistically different from one another, it should be pointed out that these "time in quadrant values" were still below the chance level of 30 s (120 s divided by four quadrants) and thus are of limited physiological significance. Members of the Nle[1]-YI and Nle[1]-YIH groups (Fig. 2B) exhibited means of 36.3 ± 1.7 and 39.6 ± 3.7 s, respectively, in the target quadrant, statistically above chance level but not different from one another. Even though the Nle[1]-YIHP- and Nle[1]-AngIV-treated groups differed with means of 47.2 ± 2.2 and 56.0 ± 4.0 s, respectively, both groups exhibited effective search strategies and demonstrated persistence to remain in the target quadrant. The Nle[1]-AngIV-treated rats (56.0 ± 4.0 s) did not differ from the unimpaired vehicle control group (58.2 ± 3.5 s) (Fig. 2A). Members of the three groups treated with 0.1, 1, or 5 nmol of Nle[1]-YI (Fig. 2C) did show differences in persistence to remain in the target quadrant (24.2 ± 3.1, 36.3 ± 1.7, and 46.6 ± 2.9 s, respectively) from those for the group treated with 5 nmol, indicating the greatest persistence.

To evaluate the possible impact of scopolamine or the applied peptides on motor function, swim speeds were measured on day 8 of acquisition training. No differences in swim speeds were evident among the seven experimental groups presented in Fig. 2, A and B ($F = 2.01$, $df = 6/49$, $p > 0.05$). Swim speeds (mean ± S.E.M. after each analog) are presented for rats pretreated with scopolamine followed by Nle[1]-Y (0.33 ± 0.02 m/s), Nle[1]-YI (0.34 ± 0.03 m/s), Nle[1]-YIH (0.34 ± 0.05 m/s), Nle[1]-YIHP (0.36 ± 0.02 m/s), or Nle[1]-AngIV (0.39 ± 0.02 m/s). Swim speeds for the scopolamine followed by aCSF and aCSF followed by aCSF groups were 0.34 ± 0.02 and 0.39 ± 0.02 m/s, respectively. There were no differences in swim speeds among the 0.1-, 1-, or 5-nmol Nle[1]-YI groups: 0.35 ± 0.03, 0.34 ± 0.03, and 0.36 ± 0.02 m/s, respectively.

Effects on Synaptogenesis. The cognitive-enhancing ability of Nle[1]-AngIV-related peptides led us to predict that these peptides could be expected to promote changes in synaptic connectivity resulting in augmented synaptic communication. The known linkage of improved synaptic communication to the expansion of dendritic spine numbers and increased head size encouraged an evaluation of potential changes in spine morphology. To test this hypothesis, we examined the effect of these peptides on spinogenesis. As anticipated, the data presented in Fig. 3A indicate that the average number of dendritic spines/50 μm of dendrite length after 5 days of treatment with 1 pM Nle[1]-AngIV or various C-terminal truncated peptides increased significantly. Nle[1]-AngIV (mean spine numbers = 32.4) treatment induced a 103% increase in spine numbers over control (mean spine numbers = 16.0). A similar increase was evident with the Nle[1]-YIHP (mean spine numbers = 31.4). Treatment with Nle[1]-YIH (mean spine numbers = 23.3), with Nle[1]-YI (mean spine numbers = 26.5), and, to a lesser extent, with Nle[1]-Y (mean spine numbers = 21.9) also yielded an increase in spine numbers compared with control.

Treatment with the AngIV-related, but cognitively inactive, peptide YIHPF (Wright et al., 1999), which was included as a negative control, produced no change in spine numbers (mean spine numbers = 16.0). The positive control, brain-derived neurotrophic factor (BDNF) (50 μM), a known stim-

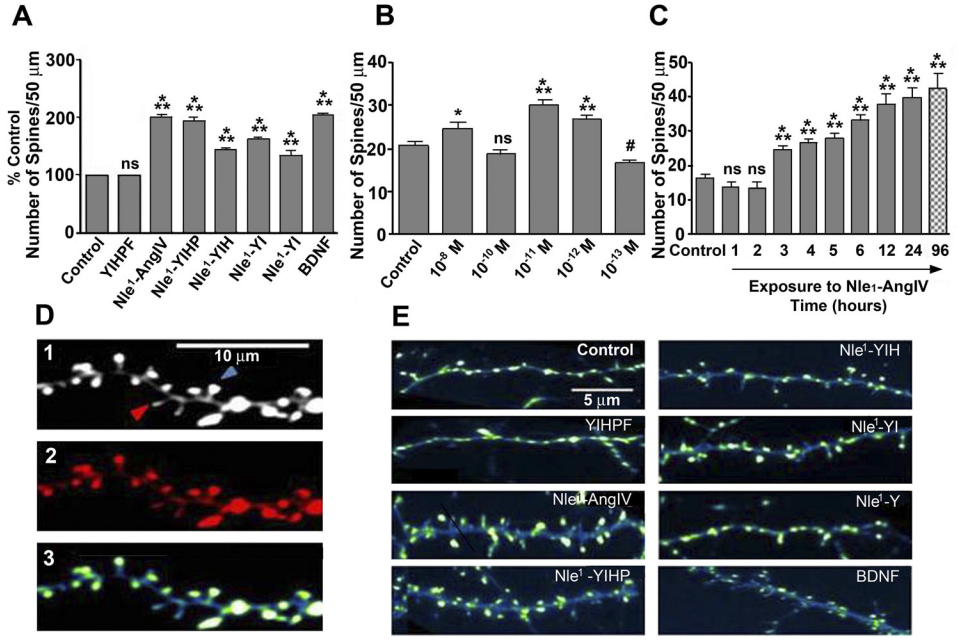

Fig. 3. Effect of C-terminal truncated peptides on the number of dendritic spines per segment of dendrite. A, percentage increase in the number of spines, marked with mRFP-β-actin, per 50 μm of dendrite in dissociated rat hippocampal neurons compared with vehicle-treated control dendrites on in vitro day 12. Cells were treated for 5 days starting at day 7 in culture. BDNF was included as a positive control and YIHPF, an inactive AngIV analog, was included as a negative control. Mean ± S.E.M., ***, $p < 0.001$; *, $p < 0.05$; ns, not significant. $n = 200$. B, dose response for the shortest active fragment, Nle[1]-YI, indicating the number of treatment-induced spines/50-μm dendrite length in hippocampal neurons. Mean ± S.E.M. C, time course response for Nle[1]-AngIV-treated neurons. The *x*-axis represents the time neurons were exposed to the peptide. D, representative image of a dendritic segment shown in gray scale (1) to indicate different spine morphologies (the red arrow is pointing to an immature thin spine and the blue arrow to a mature mushroom spine) and in red (2) to illustrate mRFP-β-actin labeling; in the same segment is converted to the pseudo-color green-fire blue (3), which aids in visualization of actin enrichment in the postsynaptic spine (yellow). E, pseudocolor photomicrographs of representative dendrite segments. Yellow-green staining is mRFP-β-actin.

ulant of spinogenesis, induced an increase in spine numbers (mean spine numbers = 32.7) similar to that observed with Nle[1]-AngIV. Data in Fig. 3A were normalized to the number of spines observed for the nontreated controls used in each experiment. Figure 3D represents an original capture image in black and white (1), pseudo-colored red (2), and pseudo-color green-fire blue to demonstrate actin enrichment in the postsynaptic spine (3) images of the same dendrite segment. Representative pseudo-color photomicrographs of dendritic segments from each experimental group showing actin-labeled dendritic spines (yellow-green extensions) are presented in Fig. 3E.

The dose-response relationship observed for Nle[1]-YI to overcome scopolamine-induced amnesia encouraged us to evaluate the effect of dose on the ability of Nle[1]-YI to induce spines in dissociated hippocampal cultures (Fig. 3B). This study determined that the 10^{-11} and 10^{-12} M doses of Nle[1]-YI (mean spine numbers = 30.2 and 26.3, respectively) produced the most robust effects. Both higher and lower doses produced either no or only modest changes in spine numbers compared with untreated controls. Overall, the dose-response curve appeared hormetic in nature, which is a common feature of many hormone/receptor interactions (Calabrese and Baldwin, 2003).

The temporal pattern of change in spine numbers in response to Nle[1]-AngIV exposure is shown in Fig. 3C. These data indicate that significant changes in spine numbers are not apparent until 3 h of Nle[1]-AngIV exposure with maximum alterations being observed at 24 h of treatment. A pulse-washout experiment in which dissociated neurons were treated with 1 pM Nle[1]-AngIV for only 30 min resulted in a significant increase in spines when observed 96 h later [control 16.7 ± 0.7 spines/50 μm of dendrite segment (mean ± S.E.M., $n = 125$) versus treated 24.0 ± 0.9 ($n = 50$)].

The width of the spine head often reflects the size of the postsynaptic density, the abundance of postsynaptic receptors, and the receptivity of the postsynaptic neuron to presynaptic signals (Kennedy et al., 2005). Thus, it is not surprising that a concomitant enlargement of spine head size (width) often accompanies increases in spine numbers. On the basis of this known association, the ability of the Nle[1]-AngIV-related peptides to alter dendritic spine head size was evaluated. Measurements of head width were taken from thin and mushroom spines within treatment groups. A thin spine is defined as having a small head size that is not wider than the shaft, and a mushroom spine is defined as having a thicker, shorter neck, and a head width that exceeds its neck and is enriched in actin. A pattern similar to that reported above for spine numbers was obtained for spine head size, the only exception being spines from Nle[1]-Y-treated cells, which were not different from the negative or vehicle controls (Fig. 4A). Analysis of these data indicated that the largest spine heads were apparent in the Nle[1]-AngIV group (mean spine head width = 1.30 μm; 194% of control); although spine head size was smallest in the vehicle control (mean spine head width = 0.67 μm), negative control (mean spine head width = 0.72 μm), and Nle[1]-Y-treated (mean spine head width = 0.72 μm) groups, which were not statistically different from one another. The Nle[1]-YIHP-treated (mean spine head width = 1.12 μm), Nle[1]-YIH-treated (mean spine head width = 1.12 μm), and Nle[1]-YI -treated (mean spine head width = 1.03 μm) groups were intermediate in terms of spine head size and statistically different from controls ($p < 0.005$).

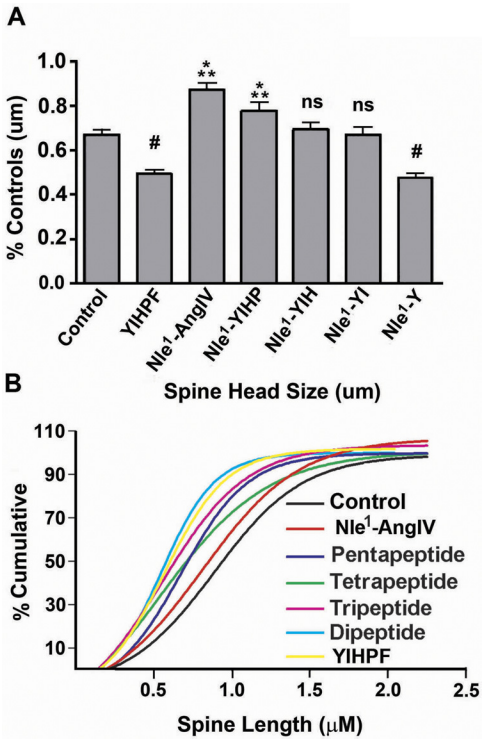

Fig. 4. Effect of C-terminal truncated peptides on dendritic spine head size and length. A, percentage increases in spine head size after drug treatment compared with vehicle dendrites. Mean ± S.E.M. ***, $p < 0.001$; #, $p < 0.05$ from control; ns, not significant. $n = 200$. B, cumulative distribution curve showing the spine length distribution for treatment groups from a representative experiment. Data were fit to a Boltzmann distribution. The inactive AngIV analog YIHPF was included as a negative control.

A common feature of dendritic spines is a maturation process in which they change from long thin structures with little or no discernible heads and few postsynaptic receptors to spines with large heads, which are both wide and thick and enriched with postsynaptic receptors (Lee et al., 2004b). As part of an effort to quantify spine shape changes initiated by Nle[1]-AngIV-related peptides, alterations in total spine length were evaluated after peptide treatment. It should be noted that total spine length included both shaft neck length plus head thickness. Figure 4B presents cumulative distribution data for each experimental group with respect to total spine length. Data from each treatment group fit a standard Boltzmann distribution with curves that had r^2 values >0.99. As expected, spines from the control group had the longest median length ($V_{50} = 0.84$ μm) and were composed primarily of thin spine shafts (Fig. 4B). The morphology of the spines seen in the control group, with small heads and long thin spine shafts, is characteristic of immature spines (Lee et al., 2004b). The general pattern for the drug-treated groups was decreasing spine neck length and increasing head thickness (length) as the procognitive capability of the peptide increased. As such, spines from neurons treated with Nle[1]-AngIV had short shaft necks with the thickness of the heads accounting for most of the total spine length (Fig. 4B) ($V_{50} = 0.77$ μm; $p < 0.05$ compared with control). The Nle[1]-YIHP-treated group exhibited the next longest spines (Fig. 4B) of the treated groups ($V_{50} = 0.62$ μm; $p < 0.05$ compared with control), which were again found to be composed almost exclusively of a thick spine head (Fig. 4A). Although no

statistical differences in length were observed among the Nle[1]-YIH-treated (V_{50} = 0.50 μm), Nle[1]-YI-treated (V_{50} = 0.52 μm), and Nle[1]-Y-treated (V_{50} = 0.51 μm) groups compared with controls, the shape of spines in the Nle[1]-YIH and Nle[1]-YI groups were markedly different from the Nle[1]-Y-treated group (Fig. 4B). Like the Nle[1]-AngIV and Nle[1]-YIHP groups, the Nle[1]-YIH and Nle[1]-YI groups possessed spines with thick heads and short shafts, whereas the Nle[1]-Y group revealed short spines that either appeared as thin filopodia or as swellings of the dendritic shaft. Morphology similar to the Nle[1]-Y group was noted for neurons treated with the cognitively inactive pentapeptide YIHPF (Fig. 4B) (V_{50} = 0.53 μm).

To evaluate the functionality and transmitter signature of the newly formed spines, mRFP-β-actin-labeled neurons were immunostained for synapsin, a universal marker of presynaptic active zones (Ferreira and Rapoport, 2002) or VGLUT1, the vesicular transporter for glutamate that is found presynaptically at glutamatergic synapses (Balschun et al.). The hippocampal cultures used in these studies were heterogeneous with regard to cell type and neuronal size represented. The neurons evaluated for spine characteristics were limited to spiny neurons that were pyramid-like (~20 μm cell bodies and asymmetric dendrite distribution). The results presented in Fig. 5A indicate that the ratio of synapsin-labeled synapses, juxtaposed to mRFP-β-actin-labeled spines, remained a constant whether found in control neurons or those treated with truncated peptides. The colocalization of mRFP-β-actin-labeled dendritic spines (red) with synapsin (green) in control and Nle[1]-AngIV-treated groups can be seen in Fig. 5D. The data presented in Fig. 5B indicate colocalization of mRFP-β-actin and α-VGLUT1, thus demonstrating that the proportion of spines that were juxtaposed to glutamatergic synapses was independent of treatment. This colocalization is illustrated in photomicrographs (Fig. 5E) for the control and Nle[1]-AngIV-treated groups (mRFP-β-actin, red; VGLUT1, green). Thus, it appears that the new spines elaborated after treatment formed functional excitatory synapses.

In concert with the immunohistochemical studies, we evaluated spontaneous synaptic activity in Nle[1]-AngIV-treated hippocampal neurons using whole-cell patch-clamp techniques. Treatment with 1 pM Nle[1]-AngIV was found to increase the frequency of mEPSCs by 72% (5.27 ± 0.43 Hz, $p > 0.001$, $n = 33$) above control levels (3.06 ± 0.23 Hz, $n = 25$). This increase is reminiscent of the 101% increase in spine numbers observed for Nle[1]-AngIV treatment and supports the conclusion that the new spines instigated by Nle[1]-AngIV have functional synapses (Fig. 5, C and F).

The graded behavioral and morphological responses observed for the different peptides induced us to ask whether the in vivo procognitive potential of a compound in adult rats could be predicted from their effect on the spine architecture of neonatal hippocampal neurons in vitro. Thus, a correlation analysis was performed. In this analysis the number of spines per 50 μm of dendrite or the mean head size (width) of the spines was graphed against the latency of rats to find the submerged platform in the water maze. Two test days were examined: day 3 when large improvements in water maze learning were observed and day 8 when maximum maze performance had been achieved. Each graph was assembled from the six data points that represented the different treatment conditions (vehicle or peptides) and analyzed by linear regression. Spine number data versus test day 3 (Fig. 6A, ▲) produced a highly significant correlation (r^2 =

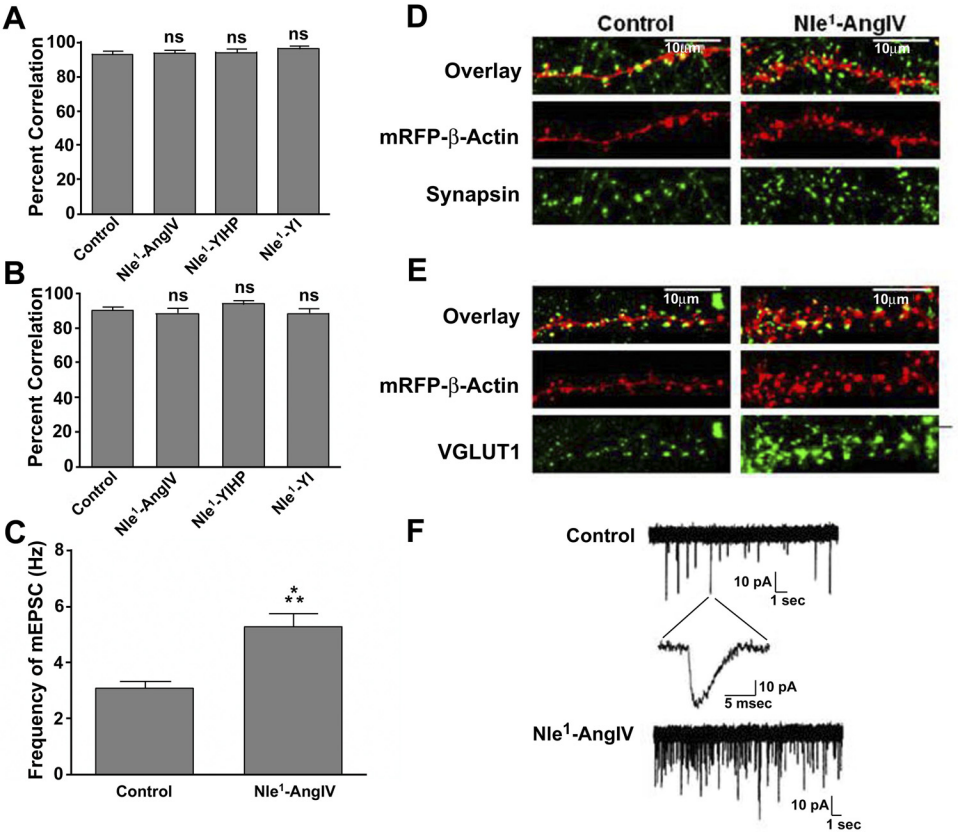

Fig. 5. Correlation between dendritic spines and active zone markers. A, percentage correlation between dendritic spines marked with mRFP-β-actin and the presynaptic active zone marker synapsin in dissociated rat hippocampal neurons on in vitro day 12. Cells were treated for 5 days starting at day 7 in culture. Cultured neurons for immunocytochemistry were untreated (vehicle control) or stimulated with 1 pM Nle[1]-AngIV, 1 pM Nle[1]-YIHP, or 1 pM Nle[1]-YI. Mean ± S.E.M., $n = 50$. One-way ANOVA indicated no differences among groups. B, percentage correlation between dendritic spines marked with mRFP-β-actin and the glutamatergic active zone marker α-VGLUT1 in dissociated rat hippocampal neurons. C, effect of Nle[1]-AngIV on the frequency of mEPSCs from dissociated hippocampal neurons. Cultured neurons for electrophysiology recordings were treated with vehicle or 1 pM Nle[1]-AngIV for 5 days before recording. Mean ± S.E.M., ***, $p < 0.001$; ns, not significant. $n = 25$ for control and 33 for Nle[1]-AngIV. D, representative dendrite segments showing juxtaposed mRFP-β-actin (red) and synapsin (green). E, representative dendrite segments showing juxtaposed mRFP-β-actin (red) and α-VGLUT1 (green). F, representative traces for control and Nle[1]-AngIV-treated neurons.

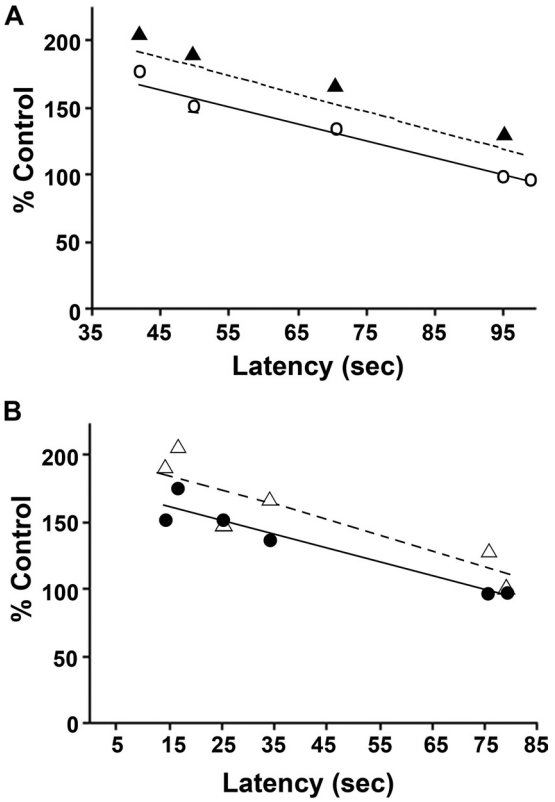

Fig. 6. Correlation analysis of water maze performance versus dendritic spine properties. The number of spines per 50 μm of dendrite or the mean head size of the spines was graphed against the latency for rats to find the submerged platform in the water maze. Two test days were examined: day 3 when learning is most active (A) and day 8 when maximum learning had occurred (B). Each graph was assembled from six data points that represented the different treatment conditions (vehicle or peptides) and analyzed by linear regression. Spine number data for test day 3 (▲) produced a highly significant correlation ($r^2 = 0.76$; $p < 0.001$). Comparison of head size to latency (○) also produced a tight linear fit ($r^2 = 0.96$; $p < 0.001$). Total spine numbers versus day 8 latency correlated significantly (△; $r^2 = 0.81$; $p < 0.001$), as did mean spine head size versus day 8 latency (●; $r^2 = 0.92$; $p < 0.001$).

0.76; $p < 0.001$). Comparison of head size to latency on day 3 (Fig. 6A, ○) also produced a tight linear fit ($r^2 = 0.96$; $p < 0.001$). These strong correlations were maintained on test day 8. Total spine numbers correlated significantly with latency on day 8 (Fig. 6B, △; $r^2 = 0.81$; $p < 0.001$), as did mean spine head size (Fig. 6B, ●; $r^2 = 0.92$; $p < 0.001$).

Discussion

The first goal of this study was to determine the minimum structural features contained within the AngIV molecule required to support its procognitive activity. The starting point was Nle^1-AngIV, an analog known to compete better than native AngIV for ^{125}I-AngIV binding sites (Sardinia et al., 1993, 1994), exhibit procognitive activity (see *Introduction*), and augment long-term potentiation (LTP) (Davis et al., 2006). Some years ago our laboratory determined that deletion of valine at the N terminus of AngIV yielded a cognitively inactive molecule (Wright et al., 1999). Thus, with Nle^1-AngIV acting as the parent molecule, successive truncations from the carboxyl terminus were made in an effort to identify the smallest active fragment. The water maze data presented indicate that the pentapeptide Nle^1-YIHP and tetrapeptide Nle^1-YIH possessed procognitive activity equivalent to that of the parent peptide Nle^1-AngIV at the same dose. To our surprise, the tripeptide Nle^1-YI at an equivalent 1-nmol dose was capable of partially reversing scopolamine-induced amnesia. Dose-response studies further revealed that Nle^1-YI was capable of complete reversal of amnesia at a higher 5-nmol dose. Hence, the effectiveness of Nle^1-YI, coupled with the ineffectiveness of Nle^1-Y, denoted the three N-terminal amino acids critical for procognitive activity.

Persistence to remain in the target quadrant during probe trials has been used to assess the relative strength of the learning achieved during maze training (Lopez et al., 2009). Results from probe trials indicated that sequential removal of amino acids from the C terminus of Nle^1-AngIV progressively reduced the search time in the target quadrant, thus reflecting the overall level of water maze learning.

Careful inspection of the acquisition data indicated that none of the peptide-treated groups exhibited shorter latencies than the scopolamine-impaired group on day 1 of training. Significant differences (i.e., improved learning) among the impaired group and the treated groups were not apparent until days 2 to 4 of acquisition, depending on the compound applied. The lack of improvement seen on day 1 of training, the improvement seen as early as day 2, and the short interval between scopolamine application, peptide application, and testing suggest that molecular events, probably translation and/or transcription, may be required for the observed cognitive improvement to manifest. This hypothesis is further supported by data indicating that changes in dendritic spine morphology were not evident until 3 to 4 h after Nle^1-AngIV application and as such would not be apparent after the first day's infusion.

The unexpected finding that Nle^1-YI possessed marked procognitive activity is important for two reasons related to our goal of producing therapeutically relevant, BBB-permeable, molecules. First, one of several features typical of molecules that are permeable to the BBB is small size, an obvious property of the peptide. Second, a synthetic template of only three amino acids significantly limits the number of possible structural modifications that need to be evaluated to produce the most efficacious compound.

The second major objective of the present investigation was to identify the mechanism that underlies the procognitive ability of these compounds. An important insight into a possible mechanism was gleaned from past studies (Kramár et al., 2001; Davis et al., 2006), indicating that Nle^1-AngIV augmented LTP in hippocampal slices. LTP is typically accompanied by changes in dendritic architecture (Kasai et al., 2010) that manifest as expanded dendritic arborization, increased numbers of dendritic spines, and an enlargement of the spine heads that house the postsynaptic receptive machinery. Furthermore, changes in spine architecture appear to be a critical contributor to memory stabilization (Xu et al., 2009). This linkage between memory stability, LTP, and altered dendritic morphology led us to hypothesize that active C-terminal truncated peptides should induce concomitant changes in dendritic spine structure. Morphological analysis revealed that treatment of dissociated hippocampal cell cultures with Nle^1-AngIV and each of the C-terminal truncated analogs except the Nle^1-Y, significantly increased both the number of dendritic spines and the size of the spine head.

Although spine length generally increased in concert with the procognitive activity of the test peptide the spine shaft length markedly decreased. This difference comparing treated versus control groups may reflect spine maturation (Lee et al., 2004b). The spines from neurons treated with procognitive peptides generally appeared mushroom-shaped with wide and thick (longer) heads, attributes correlated with mature spines that have strengthened synaptic connectivity (Saneyoshi et al., 2010). In contrast, the spines seen in the control group, although long, had thinner shafts, suggesting an earlier stage of maturation. Thus, it appears that treatment with procognitive peptides not only stimulated an expansion of spine numbers but also hastened the maturation process. Both the negative control (YIHPF) and Nle^1-Y groups exhibited similar effects on spine shape. Although thin spines similar to those seen in the vehicle control group were also observed in both the negative control and Nle^1-Y groups, a second type of spine, which manifested as swellings on the dendrite, was apparent in these groups. Because a previous cognitive study demonstrated that the negative control, YIHPF, possessed neither cognitive enhancing nor inhibiting activity (Wright et al., 1999), the functional significance of these dendritic swellings remains unclear.

A final question posed by these studies concerned whether there is a quantitative relationship between a molecule's in vivo procognitive activity and its in vitro ability to alter dendritic spine structure. Correlational data (Fig. 6) suggest that such a relationship exists, at least for these Nle^1-AngIV-derived peptides. Because of uncertainty regarding which critical learning or spine architectural features to evaluate, four different correlations were examined. In all cases these correlations were highly significant with a comparison of maze latency at day 3 versus spine head size, yielding a correlation coefficient of 0.96. These data are consistent with the prevailing notion that learning efficiency is directly dependent on synaptic connectivity and highlight the predictive value of structural dendritic spine characteristics as pertaining to spatial learning. Current studies are ongoing to verify the direct relationship between cognitive capacity and spine growth in vivo.

The experimental design of the dendritic spine study featured the use of both negative (YIHPF) and positive controls (BDNF). As expected, YIHPF failed to stimulate changes in spine number or size, and its effects were not different from those of the vehicle. BDNF, widely recognized as a strong potentiator of dendritic spine plasticity and synaptic strength in hippocampal neurons (Tyler and Pozzo-Miller, 2003; von Bohlen und Halbach et al., 2008), induced alterations in spine architecture equivalent to those observed with our procognitive peptides. However, it should be noted that the concentration of BDNF required to produce equivalent increases in dendritic spines was 7 orders of magnitude greater than that needed for the Nle^1-AngIV.

To evaluate the neurotransmitter signature of newly formed dendritic spines, immunocytochemical methods were used to determine whether dendritic spines were juxtaposed to markers of presynaptic active zones. Data derived using synapsin, a general marker of presynaptic active zones (Ferreira and Rapoport, 2002), indicated that >95% of dendritic spines in the Nle^1-AngIV, pentapeptide and Nle^1-YI groups (the only groups examined) were associated with synapsin and thus presumed to possess active synapses. Not surprisingly the vast majority of the dendritic spines were also juxtaposed to active zones that stained for α-VGLUT1, the most abundant isoform of vesicular glutamate transporters in the central nervous system (Balschun et al., 2010). Although the ratio of synapsin and α-VGLUT1 staining to mRFP-β-actin staining was independent of treatment, the absolute number of glutamatergic contacts was less than the total number of synaptic contacts. This result suggests that some of the newly formed spines were receptive to nonglutamate signaling. It is attractive to speculate that these additional contacts could be with either cholinergic neurons that are known to be concentrated in the stratum oriens (Towart et al., 2003), or abundant GABAergic neurons (Klausberger, 2009). Electrophysiological methods for which mEPSCs are monitored represent an alternative or adjunctive approach for evaluating the functionality of newly formed spines (Tyler and Pozzo-Miller, 2003). As anticipated, our electrophysiological studies with Nle^1-AngIV-treated hippocampal neurons support the contention that the new dendritic spines induced by Nle^1-AngIV treatment contained functional synapses.

This study is the first to systematically evaluate C-terminal shortened Nle^1-AngIV analogs in an effort to identify the smallest Nle^1-AngIV-related molecule with substantial procognitive activity. Overall, the results indicate that fragments as small as a tetrapeptide and tripeptide are capable of facilitating the cognitive processing necessary to overcome scopolamine-induced amnesia. Moreover, it appears that the likely mechanism underlying this marked procognitive activity is augmented synaptic connectivity. Our next step in the development of AngIV-based cognitive enhancers will be to use Nle^1-YI as a template to guide the synthesis of small molecules with enhanced metabolic stability and improved permeability across the gut and blood-brain barriers. Past studies from our laboratory indicated that angiotensin-related peptides are primarily degraded through the action of exopeptidases (Abhold and Harding, 1988). Thus, current synthetic efforts are being directed at stabilizing the amino and carboxyl termini of Nle^1-YI and Nle^1-YIH while maintaining the desired procognitive activity. Although still in progress, these studies indicate that metabolically stable analogs with excellent procognitive activity can be produced using several synthetic strategies (J. W. Harding and J. W. Wright, unpublished data).

Acknowledgments

We thank Megan Vento, Lyndsey Hepworth, and Megan Wilson for help with the behavioral testing protocols; Ruth Day and Jeanne Jensen for excellent secretarial and editorial assistance; and Kay Shi for excellent technical assistance.

Authorship Contributions

Participated in research design: Benoist, Wright, Appleyard, Wayman, and Harding.

Conducted experiments: Benoist and Zhu.

Contributed new reagents or analytic tools: Harding.

Performed data analysis: Benoist, Wright, and Harding.

Wrote or contributed to the writing of the manuscript: Benoist, Wright, Appleyard, Wayman, and Harding.

References

Abhold RH and Harding JW (1988) Metabolism of angiotensins II and III by membrane-bound peptidases from rat brain. *J Pharmacol Exp Ther* **245:**171–177.

Balschun D, Moechars D, Callaerts-Vegh Z, Vermaercke B, Van Acker N, Andries L, and D'Hooge R (2010) Vesicular glutamate transporter VGLUT1 has a role in

hippocampal long-term potentiation and spatial reversal learning. *Cereb Cortex* **20:**684–693.
Braszko JJ, Kupryszewski G, Witczuk B, and Wiśniewski K (1988) Angiotensin II-(3-8)-hexapeptide affects motor activity, performance of passive avoidance and a conditioned avoidance response in rats. *Neuroscience* **27:**777–783.
Calabrese EJ and Baldwin LA (2003) The hormetic dose-response model is more common than the threshold model in toxicology. *Toxicol Sci* **71:**246–250.
Chai SY, Bastias MA, Clune EF, Matsacos DJ, Mustafa T, Lee JH, McDowall SG, Paxinos G, Mendelsohn FA, and Albiston AL (2000) Distribution of angiotensin IV binding sites (AT4 receptor) in the human forebrain, midbrain and pons as visualised by in vitro receptor autoradiography. *J Chem Neuroanat* **20:**339–348.
Davis CJ, Kramár EA, De A, Meighan PC, Simasko SM, Wright JW, and Harding JW (2006) AT4 receptor activation increases intracellular calcium influx and induces a non-*N*-methyl-D-aspartate dependent form of long-term potentiation. *Neuroscience* **137:**1369–1379.
De Bundel D, Demaegdt H, Lahoutte T, Caveliers V, Kersemans K, Ceulemans AG, Vauquelin G, Clinckers R, Vanderheyden P, Michotte Y, et al. (2010) Involvement of the AT1 receptor subtype in the effects of angiotensin IV and LVV-haemorphin 7 on hippocampal neurotransmitter levels and spatial working memory. *J Neurochem* **112:**1223–1234.
De Bundel D, Smolders I, Vanderheyden P, and Michotte Y (2008) Ang II and Ang IV: unraveling the mechanism of action on synaptic plasticity, memory, and epilepsy. *CNS Neurosci Ther* **14:**315–339.
Faure S, Chapot R, Tallet D, Javellaud J, Achard JM, and Oudart N (2006) Cerebroprotective effect of angiotensin IV in experimental ischemic stroke in the rat mediated by AT_4 receptors. *J Physiol Pharmacol* **57:**329–342.
Ferreira A and Rapoport M (2002) The synapsins: beyond the regulation of neurotransmitter release. *Cell Mol Life Sci* **59:**589–595.
Fisher A, Pittel Z, Haring R, Bar-Ner N, Kliger-Spatz M, Natan N, Egozi I, Sonego H, Marcovitch I, and Brandeis R (2003) M1 muscarinic agonists can modulate some of the hallmarks in Alzheimer's disease: implications in future therapy. *J Mol Neurosci* **20:**349–356.
Fyhrquist F and Saijonmaa O (2008) Renin-angiotensin system revisited. *J Intern Med* **264:**224–236.
Gard PR (2004) Angiotensin as a target for the treatment of Alzheimer's disease, anxiety and depression. *Expert Opin Ther Targets* **8:**7–14.
Gard PR (2008) Cognitive-enhancing effects of angiotensin IV. *BMC Neurosci* **9 (Suppl 2):**S15.
Harding JW, Cook VI, Miller-Wing AV, Hanesworth JM, Sardinia MF, Hall KL, Stobb JW, Swanson GN, Coleman JK, and Wright JW (1992) Identification of an AII(3–8) [AIV] binding site in guinea pig hippocampus. *Brain Res* **583:**340–343.
Kasai H, Fukuda M, Watanabe S, Hayashi-Takagi A, and Noguchi J (2010) Structural dynamics of dendritic spines in memory and cognition. *Trends Neurosci* **33:**121–129.
Kennedy MB, Beale HC, Carlisle HJ, and Washburn LR (2005) Integration of biochemical signalling in spines. *Nat Rev Neurosci* **6:**423–434.
Klausberger T (2009) GABAergic interneurons targeting dendrites of pyramidal cells in the CA1 area of the hippocampus. *Eur J Neurosci* **30:**947–957.
Kramár EA, Armstrong DL, Ikeda S, Wayner MJ, Harding JW, and Wright JW (2001) The effects of angiotensin IV analogs on long-term potentiation within the CA1 region of the hippocampus in vitro. *Brain Res* **897:**114–121.
Kramár EA, Harding JW, and Wright JW (1997) Angiotensin II- and IV-induced changes in cerebral blood flow. Roles of AT1, AT2, and AT4 receptor subtypes. *Regul Pept* **68:**131–138.
Lee J, Albiston AL, Allen AM, Mendelsohn FA, Ping SE, Barrett GL, Murphy M, Morris MJ, McDowall SG, and Chai SY (2004a) Effect of I.C.V. injection of AT4 receptor ligands, NLE1-angiotensin IV and LVV-hemorphin 7, on spatial learning in rats. *Neuroscience* **124:**341–349.
Lee KJ, Kim H, Kim TS, Park SH, and Rhyu IJ (2004b) Morphological analysis of spine shapes of Purkinje cell dendrites in the rat cerebellum using high-voltage electron microscopy. *Neurosci Lett* **359:**21–24.
Lopez J, Wolff M, Lecourtier L, Cosquer B, Bontempi B, Dalrymple-Alford J, and Cassel JC (2009) The intralaminar thalamic nuclei contribute to remote spatial memory. *J Neurosci* **29:**3302–3306.
Meijering E, Jacob M, Sarria JC, Steiner P, Hirling H, and Unser M (2004) Design and validation of a tool for neurite tracing and analysis in fluorescence microscopy images. *Cytometry A* **58:**167–176.
Mustafa T, Lee JH, Chai SY, Albiston AL, McDowall SG, and Mendelsohn FA (2001) Bioactive angiotensin peptides: focus on angiotensin IV. *J Renin Angiotensin Aldosterone Syst* **2:**205–210.
Pederson ES, Krishnan R, Harding JW, and Wright JW (2001) A role for the angiotensin AT4 receptor subtype in overcoming scopolamine-induced spatial memory deficits. *Regul Pept* **102:**147–156.
Saneyoshi T, Fortin DA, and Soderling TR (2010) Regulation of spine and synapse formation by activity-dependent intracellular signaling pathways. *Curr Opin Neurobiol* **20:**108–115.
Sardinia MF, Hanesworth JM, Krebs LT, and Harding JW (1993) AT4 receptor binding characteristics: D-amino acid- and glycine-substituted peptides. *Peptides* **14:**949–954.
Sardinia MF, Hanesworth JM, Krishnan F, and Harding JW (1994) AT4 receptor structure-binding relationship: N-terminal-modified angiotensin IV analogues. *Peptides* **15:**1399–1406.
Stubley-Weatherly L, Harding JW, and Wright JW (1996) Effects of discrete kainic acid-induced hippocampal lesions on spatial and contextual learning and memory in rats. *Brain Res* **716:**29–38.
Towart LA, Alves SE, Znamensky V, Hayashi S, McEwen BS, and Milner TA (2003) Subcellular relationships between cholinergic terminals and estrogen receptor-alpha in the dorsal hippocampus. *J Comp Neurol* **463:**390–401.
Tyler WJ and Pozzo-Miller L (2003) Miniature synaptic transmission and BDNF modulate dendritic spine growth and form in rat CA1 neurones. *J Physiol* **553:**497–509.
Vanderheyden PM (2009) From angiotensin IV binding site to AT4 receptor. *Mol Cell Endocrinol* **302:**159–166.
von Bohlen und Halbach O (2003) Angiotensin IV in the central nervous system. *Cell Tissue Res* **311:**1–9.
von Bohlen und Halbach O and Albrecht D (2006) The CNS renin-angiotensin system. *Cell Tissue Res* **326:**599–616.
von Bohlen und Halbach O, Minichiello L, and Unsicker K (2008) TrkB but not trkC receptors are necessary for postnatal maintenance of hippocampal spines. *Neurobiol Aging* **29:**1247–1255.
Wayman GA, Davare M, Ando H, Fortin D, Varlamova O, Cheng HY, Marks D, Obrietan K, Soderling TR, Goodman RH, et al. (2008) An activity-regulated microRNA controls dendritic plasticity by down-regulating p250GAP. *Proc Natl Acad Sci USA* **105:**9093–9098.
Wright JW, Clemens JA, Panetta JA, Smalstig EB, Weatherly LA, Kramár EA, Pederson ES, Mungall BH, and Harding JW (1996) Effects of LY231617 and angiotensin IV on ischemia-induced deficits in circular water maze and passive avoidance performance in rats. *Brain Res* **717:**1–11.
Wright JW and Harding JW (2008) The angiotensin AT4 receptor subtype as a target for the treatment of memory dysfunction associated with Alzheimer's disease. *J Renin Angiotensin Aldosterone Syst* **9:**226–237.
Wright JW and Harding JW (2010) The brain RAS and Alzheimer's disease. *Exp Neurol* **223:**326–333.
Wright JW, Stubley L, Pederson ES, Kramár EA, Hanesworth JM, and Harding JW (1999) Contributions of the brain angiotensin IV-AT4 receptor subtype system to spatial learning. *J Neurosci* **19:**3952–3961.
Xu T, Yu X, Perlik AJ, Tobin WF, Zweig JA, Tennant K, Jones T, and Zuo Y (2009) Rapid formation and selective stabilization of synapses for enduring motor memories. *Nature* **462:**915–919.

Address correspondence to: Dr. Joseph W. Harding, Department of Veterinary and Comparative, Anatomy, Pharmacology, and Physiology, P.O. Box 6520, Washington State University, Pullman, WA 99164-6520. E-mail: hardingj@vetmed.wsu.edu